Voronina et al., http://www.jcb.org/cgi/content/full/jcb.200809144/DC1

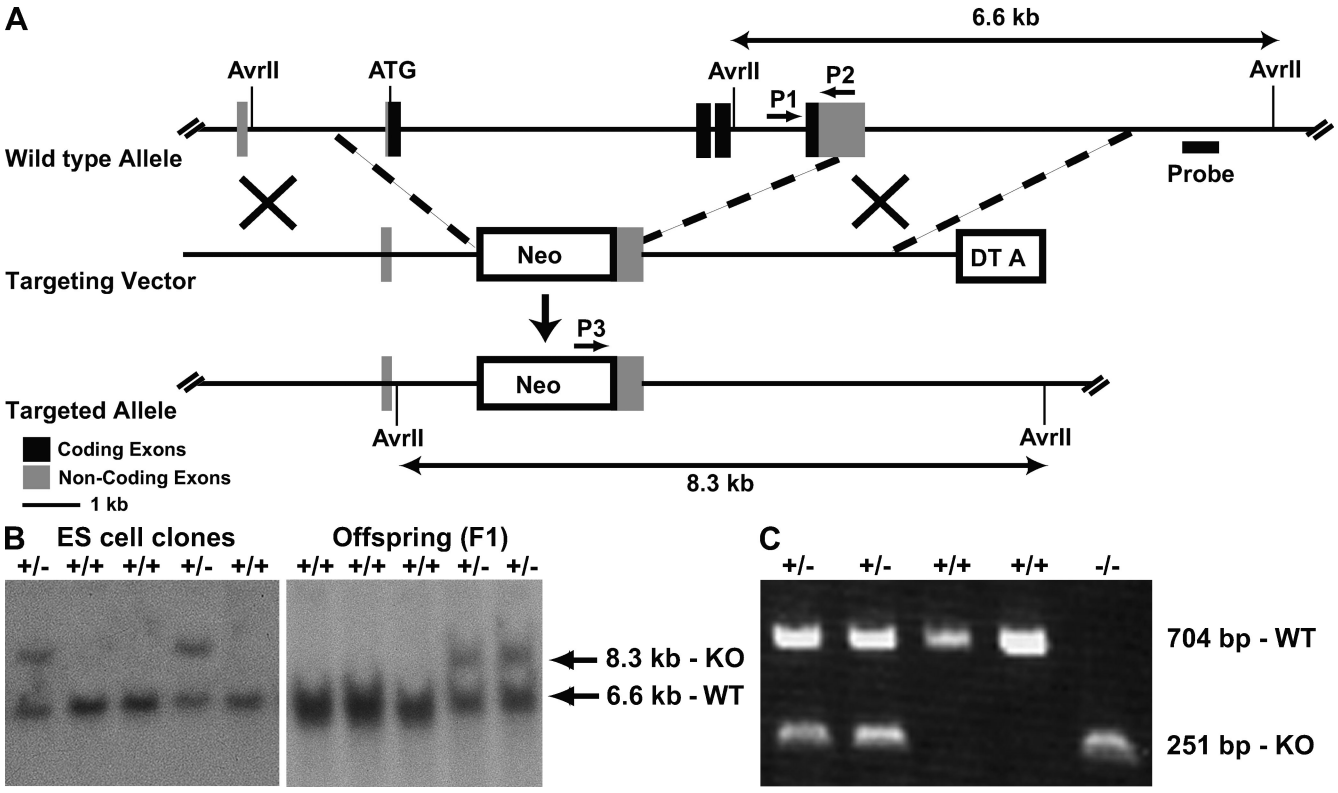

Figure S1. ***Cby* locus targeting.** (A) Schematic representation of the mouse *Cby* locus and targeting construct. The *Cby* gene consists of four coding exons, which were entirely deleted in the disrupted allele. The open boxes in the targeting vector represent the phosphoglycerate kinase–neomycin (Neo) and diphtheria toxin A (DT A) cassettes. The location of the 3′ flanking probe used for Southern blot analysis (horizontal black bar) and primers for PCR genotyping (short arrows) is indicated. (B) Southern blot analysis of embryonic stem (ES) cell lines after homologous recombination and F1 offspring from chimeric mice. The 3′ probe shown in A was used for hybridization with tail DNAs digested with AvrII. The wild-type (WT) allele generates a 6.6-kb band, whereas the targeted allele produces an 8.3-kb band. (C) PCR genotyping of weaning-age pups from a cross of $Cby^{+/-}$ mice. The primer set P1 and P2 in A detects the wild-type allele (704 bp), whereas the primers P3 and P2 amplify the knockout (KO) allele (251 bp).

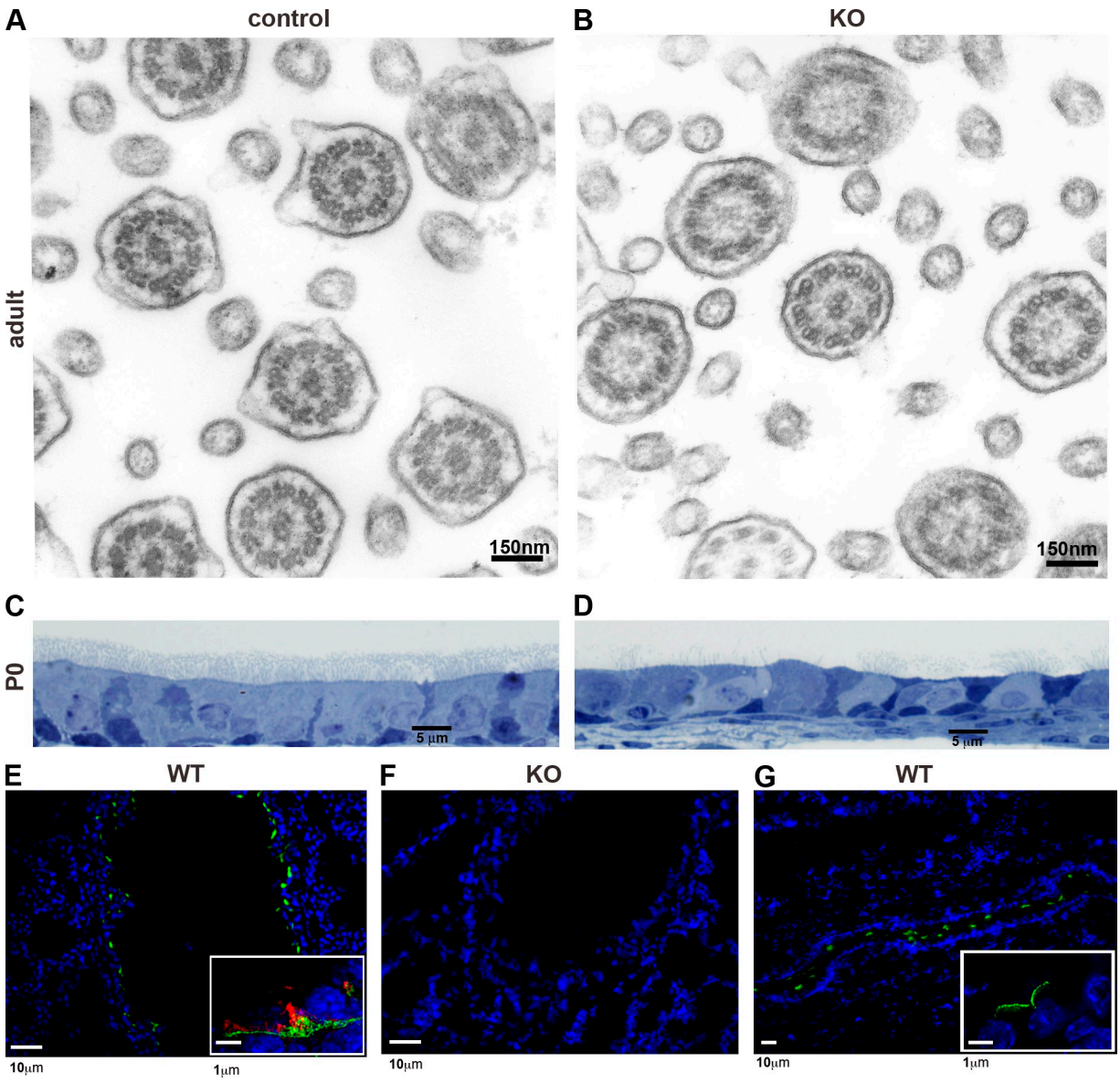

Figure S2. **Ultrastructure of the adult bronchial cilia, a paucity of nasal cilia in newborn mice, and Cby expression in embryonic lung and esophageal epithelia at E18.5.** (A and B) TEM of cross sections of motile bronchial cilia from *Cby*$^{+/+}$ (A) and *Cby*$^{-/-}$ (B) adult mice. (C and D) Toluidine blue–stained 1-μm sections of the nasal epithelium from *Cby*$^{+/-}$ (C) and *Cby*$^{-/-}$ (D) neonates. (E) E18.5 *Cby*$^{+/+}$ bronchial airway stained with Cby antibody (green). The inset shows a high magnification view of double immunostaining for Cby (green) and acetylated α-tubulin (red). (F) E18.5 *Cby*$^{-/-}$ bronchial airway stained with Cby antibody. (G) Longitudinal sections of E18.5 *Cby*$^{+/+}$ esophagus stained with Cby antibody (green). The inset is a high magnification of Cby staining. Nuclei were counterstained with DAPI. WT, wild type; KO, knockout.

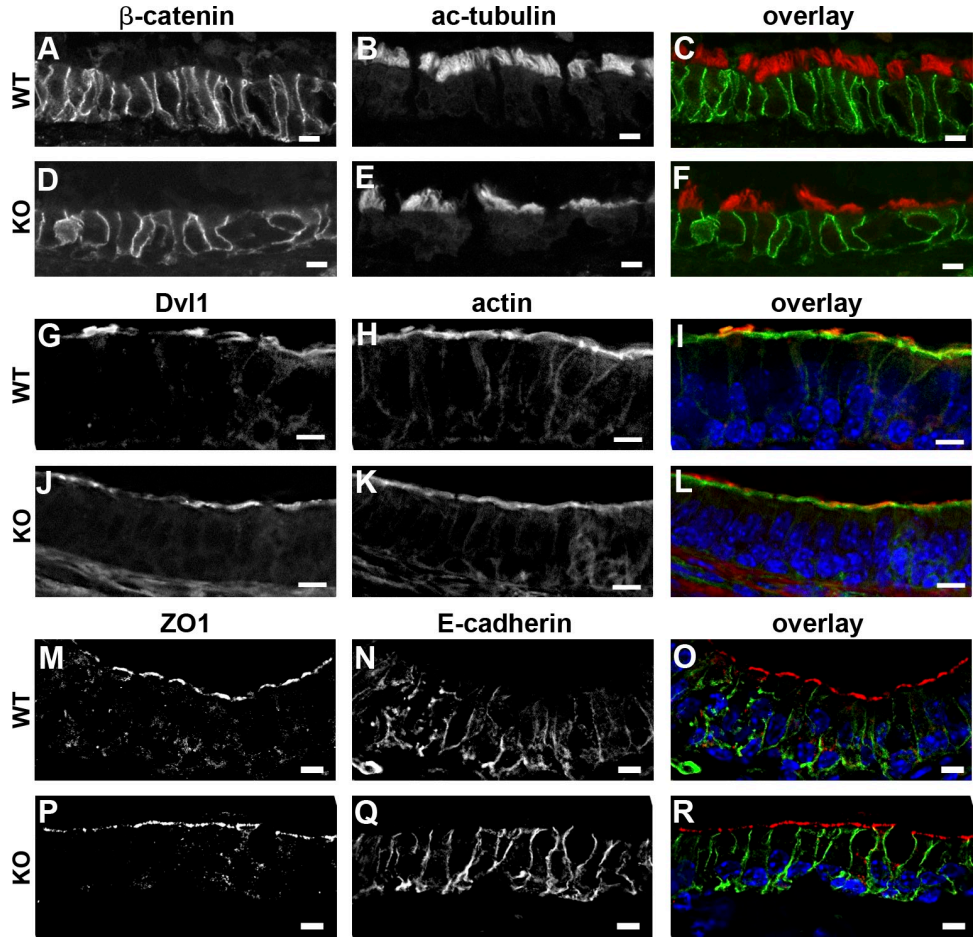

Figure S3. **Localization of β-catenin, Dvl, and apical-basal markers remains unchanged in the nasal epithelium of *Cby*$^{-/-}$ mice.** (A–F) Cross sections of the nasal epithelium from *Cby*$^{+/+}$ (A–C) and *Cby*$^{-/-}$ (D–F) adult mice were double-stained with β-catenin (A and D) and acetylated α-tubulin (ac-tubulin; B and E) antibodies. The merged images of β-catenin (green) and acetylated α-tubulin (red) are shown (C and F). (G–L) Cross sections of the nasal epithelium from *Cby*$^{+/+}$ (G–I) and *Cby*$^{-/-}$ (J–L) mice were colabeled with Dvl1 antibody (G and J) and phalloidin for actin filaments (H and K). The merged images of Dvl1 (red) and phalloidin (green) are shown (I and L). Note that extensive actin filaments are appropriately positioned at the apical surface in *Cby*$^{-/-}$ ciliated epithelial cells. (M–R) Cross sections of the nasal epithelium from *Cby*$^{+/+}$ (M–O) and *Cby*$^{-/-}$ (P–R) adult mice were doubly immunostained for ZO1 (apical marker; M and P) and epithelial cadherin (E-cadherin; basolateral marker; N and Q). The merged images of ZO1 (red) and epithelial cadherin (green) are shown (O and R). Nuclei were visualized with DAPI (I, L, O, and R). Bars: (A–F) 6 μm; (G–R) 2 μm.

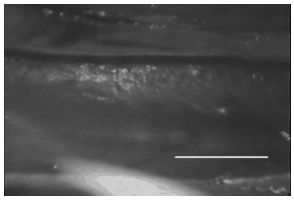

Video 1. **MCT in upper airways of control adult mice.** Mucociliary transport in nasopharynx of control mice was videotaped as described in Materials and methods. The video is shown at 15 frames/s. Bar, 500 μm.

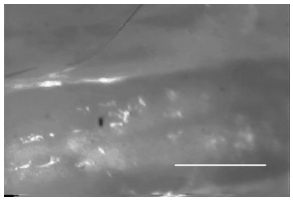

Video 2. **MCT in upper airways of adult *Cby*$^{-/-}$ mice.** Mucociliary transport in nasopharynx of *Cby*$^{-/-}$ mice was videotaped as described in Materials and methods. The video is shown at 15 frames/s. Bar, 500 μm.